Optik 126 (2015) 1150–1155

Contents lists available at ScienceDirect

Optik

journal homepage: www.elsevier.de/ijleo

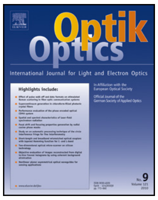

Theoretical and experimental analysis of interaction from acoustic emission on fiber Bragg grating

Mingjun Xia*, Mingshun Jiang, Qingmei Sui, Lei Jia

School of Control Science and Engineering, Shandong University, Jinan 250061, China

ARTICLE INFO

Article history:
Received 19 February 2014
Accepted 4 March 2015

Keywords:
Fiber Bragg grating
Acoustic emission detection
Gaussian-sine strain field
Interaction analysis
Intensity demodulation signal

ABSTRACT

Fiber Bragg grating (FBG) sensors have been indicated to be ideal candidates for high frequency acoustic emission (AE) detection. This paper reports that the strain fields along FBG axis generated by acoustic emission waves contain Gaussian-sine strain field distribution. Propagation matrix method is adopted to evaluate the dynamic characteristics of FBG reflection spectrum under the action of the Gaussian-sine strain field. Then, intensity demodulation signal of FBG acoustic emission detection system using 3-dB bandwidth method is theoretically simulated based on the spectrum analysis. In order to obtain accurate measurement using this system, the maximum displacement amplitude of the strain field generated by acoustic emission is explored. Furthermore, in AE experiments, Gaussian-sine waves are extracted to confirm the accuracy of the novel presentation regarding strain field generated by acoustic emission waves along FBG axis. These studies provide useful tools for acoustic emission sources position and identification by time waveform analysis.

1. Introduction

FBG sensors in acoustic emission measurements are potentially advisable in several areas, including construction, transportation and aerospace. Compared with conventional piezoelectricity sensors, FBG sensors present the characteristics: small-size, immune to electromagnetic interference and excellent embedding and multiplexing capabilities. Recently, scholars began to study acoustic emission detection sensors based on FBG to realize nondestructive healthy monitoring on composite materials [1–4]. Acoustic emission waves are multi-mode elastic waves generated by a sudden energy release, such as cracks or impacts [5]. The high frequency variation signal generates specific strain fields along FBG axis, which leads to changes of fiber grating period and refractive index. The characteristics can be used to make the position and identification of acoustic emission source so that serious damages are avoided [6–8].

Although FBG sensing system has been applied in the AE monitoring, signal transmission process is not known due to the complexity of acoustic emission waves. It is necessary to analyze the relation between the strain field distribution along the FBG and the detected signal of FBG sensing system. Previous publications investigated the response of fiber Bragg grating on acoustic emission [9,10]. Aldo Minardo et al. analyzed the response sensitivity for the uniform and Gaussian-apodized FBG to ultrasonic waves [11]. Zhuoxuan Li et al. adopted the V–I transmission matrix to analyze the FBG response to an ultrasonic wave [12]. However, these theoretical studies through numeral analysis provided limited information, as they mainly focused on sine strain field and the sensitivity of fiber Bragg grating sensors. The theoretical researches did not consider the whole optical detection system. In this paper, we present that the strain fields generated by acoustic emission waves along FBG axis contain Gaussian-sine strain filed. Furthermore, we simulate the intensity demodulation signal of the acoustic emission detection system based on experimental parameters. This makes the comparison meaningful between the theoretical simulation and AE experiments.

Section 2 deals with the acoustic emission FBG detection theory. Equations are induced to calculate dynamic reflection spectrum of FBG under the action of Gaussian-sine strain field. Meanwhile, spectral characteristics are evaluated with the effects from the acoustic emission waves. Section 3 introduces the acoustic emission detection system scheme and simulates the intensity demodulation signal of acoustic emission detection system under the action of Gaussian-sine strain field with different displacement amplitude values. In Section 4, acoustic emission experiments are done to compare the practical detection acoustic emission signal with the simulation result, which is used to confirm the accuracy of theoretical analysis. Then, conclusions are presented in Section 5.

---

* Corresponding author. Tel.: +86 18764415753.
E-mail address: xiamingjunsdu@hotmail.com (M. Xia).

http://dx.doi.org/10.1016/j.ijleo.2015.03.020
0030-4026/

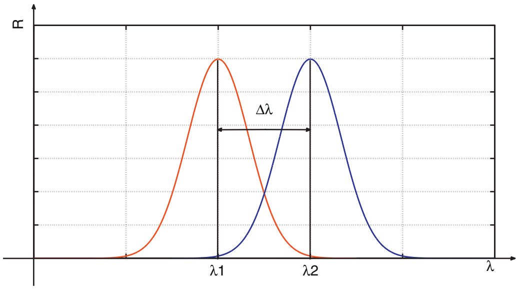

Fig. 1. Movement of FBG central wavelength.

2. Interaction theory from acoustic emission waves on FBG

2.1. FBG sensing theory

Based on the coupling mode theory, the central wavelength, which satisfies the phase-matching condition, can be reflected. The central wavelength is given by [13]

$$\lambda_{B0} = 2n_{eff0}\Lambda_0 \tag{1}$$

where λ_{B0} is the FBG central wavelength, n_{eff0} is the effective refraction index and Λ_0 is the Bragg grating period. When broadband light incidents the FBG sensor, certain wavelength light satisfying Eq. (1) would be reflected, and other light would be transmitted. Under the action of acoustic emission waves from cracks, the effective refraction index and the grating period are changed, which leads to the shift of FBG central wavelength as shown in Fig. 1.

2.2. Response of FBG to acoustic emission waves

FBG sensors are attached on the surface of the detected object, where acoustic emission source exists. When acoustic emission waves propagate along the medium, particles in the medium vibrate greatly due to the strain field distribution along FBG axis.

We make a novel presentation that the strain field generated by acoustic emission waves along the FBG axis contains Gaussian-sine strain field, which is defined as:

$$\varepsilon(z,t) = \varepsilon_m \cdot e^{-\frac{(t-t_0)^2}{a^2}} \sin\left(\frac{2\pi}{\lambda}z - 2\pi f\right), \quad z \in (0,l) \tag{2}$$

where ε_m is the strain field displacement amplitude, t_0 is the arriving time, λ and f denote the wavelength and frequency of acoustic emission waves, l is the FBG gauge length. When acoustic emission waves propagate along the FBG axis, the refractive index is changed due to the geometric effect and elasto-optic effect [14]. The effective refractive index of uniform FBG under the action of the strain field can be described as:

$$n_{eff}(z) = n_{eff0} - \Delta n \sin^2\left(\frac{\pi}{\Lambda_0}z\right) + \Delta n'(z_a), \quad z \in [0,l] \tag{3}$$

where $n_{eff}(z)$ is the FBG refractive index along the FBG axis, n_{eff0} is the refractive index of fiber core, z_a denotes the new FBG axis with the geometric effect, $\Delta n'(z_a)$ denotes the change of refractive index with the elasto-optic effect. The effective refractive modulation caused by the geometric deformation and elasto-effect can be described as [15]:

$$\begin{aligned} z_a &= z - \varepsilon_m e^{-\frac{(t-t_0)^2}{a^2}} \frac{\lambda}{2\pi} \cos\left(\frac{2\pi}{\lambda}z - 2\pi f t\right) \\ &\quad + \varepsilon_{ms} e^{-\frac{(t-t_0)^2}{a^2}} \cdot \frac{\lambda}{2\pi} \cos(2\pi f t), \quad z \in [0,l] \end{aligned} \tag{4}$$

Table 1
Simulation parameters for FBG and strain field along FBG axis.

FBG	Value	Strain field	Value
n_{eff0}	1.45	ε_{ms}	500 μ
Δn	0.002	t_0	0.18 ms
Λ_0	535 nm	a	0.000015
P_{11}	0.12	V_{a0}	1950 m/s
P_{12}	0.275	f	10 kHz
υ	0.17		

$$\Delta n'(z_a) = -\left(\frac{n_{eff0}^2}{2}\right) \cdot [P_{12} - \upsilon(P_{11}+P_{12})] \cdot \varepsilon_m \cos(z_a - 2\pi f t) \tag{5}$$

Next, the FBG effective refractive is obtained by substituting the inverse function of Eq. (4) $z = f^{-1}(z_a, t)$, and Eq. (5) in Eq. (3). This can be denoted as:

$$\begin{aligned} n_{eff}(z_a,t) &= n_{eff0} - \Delta n \sin^2\left(\frac{\pi}{\Lambda}z\right) - \left(\frac{n_{eff0}}{2}\right) \\ &\quad \cdot [P_{12} - \upsilon(P_{11}+P_{12})] \cdot \varepsilon_m \cos\left(\frac{2\pi}{\lambda}z_a - 2\pi f t\right) \end{aligned} \tag{6}$$

where $P_{i,j}$ is the stress-optic coefficient, υ is the Poisson ratio. When the FBG material and the FBG central wavelength are chosen, $P_{i,j}$ and υ are constants.

2.3. FBG spectral characteristics evaluation with Gaussian-sine strain field distribution

In the analysis above, we theoretically derived the equation of FBG refractive index under the action of Gaussian-sine strain filed. Then, the propagation matrix method [16] is employed to evaluate the FBG spectral characteristics using MatLAB program. 1 mm FBG, at the central wavelength 1550.4 nm, is assumed to be multilayer structure and the refractive index of every layer is constant. The sampling step is chosen to be 10 nm, which has to be smaller than the period of the sampled function $n_{eff}(z_a, t)$. In order to calculate the reflection spectrum, other parameters of FBG sensors and acoustic emission waves can be found in Table 1.

The ratio between the acoustic wave wavelength and the FBG gauge length is a key parameter affecting the reflection spectrum [11]. We first simulate the FBG reflection spectrum in three different ratio cases ($\lambda/l = 0.1$, 1, 10, $t = 0.17$ ms) with the parameters in Table 1. The corresponding waveform of reflection spectrum is reported in Fig. 2. Meanwhile, peak refractive index, peak wavelength, bandwidth and sidelobes level are compared in Table 2. It can be observed that when the wavelength of acoustic emission wave is larger than the FBG gauge length (ratio = 10), a significant central wavelength shift (0.28 nm) appears. At the same time, the reflection spectrum becomes broader than the natural reflection spectrum (bandwidth is 1.5 nm). Furthermore, in the second case (ratio = 1), we can observe a significant shape distortion, which is

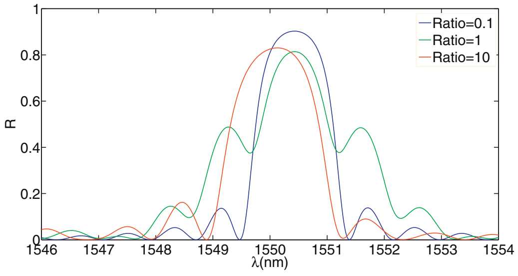

Fig. 2. FBG reflection spectrum in different ratio cases ($\lambda/l = 0.1$, 1, 10, $t = 0.17$ ms).